Thin-Film Photovoltaics Partnership Program

Third Quarterly Status Report – Year II

Covering the period of April 2, 2003 to July 1, 2003

Deliverable: Subcontract Article 3 B, **Item 10 (**ADJ-2-30630-13**)**

Project: **Fundamental Materials Research and Advanced Process Development for Thin-Film CIS-Based Photovoltaics**

P.I.: T. J. Anderson

Co-PI's: S. S. Li, O. D. Crisalle, and Rajiv K. Singh

Other Personnel: Ryan Acher, Valentin Craciun, Ozge Erdogdu, Ricardo Gomez-Gonzalez, Joshua Howard, Ryan M. Kaczynski, Lei Li Kerr, Suku Kim, Woo Kyoung Kim, Wei Liu, Matt Monroe, Seemant Rawal, Jiyon Song, Xuege Wang, and Seokhyun Yoon.

Subcontract No.: ADJ-2-30630-13

Funding Agency: National Renewal Energy Laboratory (NREL)

Program: Thin-Film Photovoltaics Partnership program

Contact Address: Tim Anderson, P.O. Box 116005, 227 Chemical Engineering Bldg., University of Florida, Gainesville FL 32611-6005, Phone: (352) 392-0882, FAX: (352) 392-9513, E-mail: tim@nersp.nerdc.ufl.edu

1 Progress on Reaction Pathways and Kinetics of $CuInSe_2$ Thin Film Growth from Bi-layer In_2Se_3/CuSe Precursor Films.

Participants: Timothy J. Anderson, Oscar D. Crisalle (Faculty Advisor), Woo Kyoung Kim, Seokhyun Yoon, Ryan Acher and Ryan Kaczynski (Graduate Research Assistant)

1.1 Objectives

In-situ study of the reaction pathways and kinetics of $CuInSe_2$ formation from bi-layer In_2Se_3/CuSe precursor film using time-resolved high temperature X-ray diffraction.

1.2 Accomplishments during the current quarter

1.2.1 Preparation of precursor films

Bi-layer In_2Se_3/CuSe precursor films were grown on the sodium-free thin(0.4mm) glass substrates in the PMEE (Plasma-assisted Migration Enhanced Epitaxy) reactor. The crystalline In_2Se_3 bottom layer was grown with a substrate temperature of approximately 400°C. The crystalline CuSe top layer was deposited on the as-grown In_2Se_3 layer at lower substrate temperature condition (~150°C) to minimize any potential reactions between the In_2Se_3 and CuSe layers. The total thickness(~0.6□m) and the atomic composition ([Cu]/[In]~0.94 ; [Se]/[Metal] ~1.2) of bilayer precursor were measured by SEM and ICP respectively.

1.2.2 Time-resolved high temperature X-ray diffraction

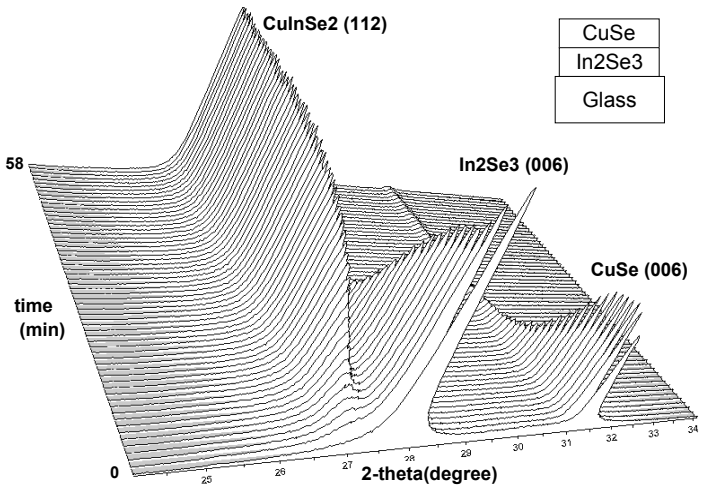

Figure 1-1. Time-resolved *in-situ* X-ray diffraction for isothermal heating at 264°C.

Time-resolved high temperature X-ray diffraction data were collected by position sensitive

detector (PSD) while the bi-layer In_2Se_3/CuSe precursor films were isothermally heated in He (flowrate~100sccm) environment. The temperature range for isothermal experiments was between 232°C and 275°C. The accurate sample temperatures were obtained by the temperature calibration method using the thermal expansion coefficient of silver. The O_2 content of outlet gas measured by O_2 analyzer was less than 0.1 ppm.

Both the consumption of CuSe and In_2Se_3 reactant phases and the formation of $CuInSe_2$ product phase were qualitatively demonstrated as shown in Figure 1-1. During the phase evolution, no intermediate phases were detected. For the quantitative analysis, the mole fractions of reactants (CuSe, In_2Se_3) and product ($CuInSe_2$) were calculated by measuring the XRD peak area (Figure 1-2). The atomic composition analysis ([Se]/[Metal]~0.95) by ICP measurement after the isothermal reaction showed the excess selenium would be evaporated during the reaction. Therefore, the following reaction can be suggested.

$$2CuSe + In_2Se_3 \rightarrow 2CuInSe_2 + Se(evaporated) \quad (1\text{-}1)$$

1.3 Activities envisioned for the next quarter

The quantitative analysis using the appropriate kinetic model will be performed.

1.4 Publications and presentations

[1] S. Kim, W.K. Kim, E.A. Payzant, R.M. Kaczynski, R.D. Acher, S. Yoon, T.J. Anderson, O.D. Crisalle, and S.S. Li, "Reaction Kinetics and Pathways of $CuInSe_2$ Growth from Bilayer Precursor Films: Time-resolved High Temperature X-ray Diffraction Analysis", *Journal of Vacuum Sciecne and Technology A (submitted).*

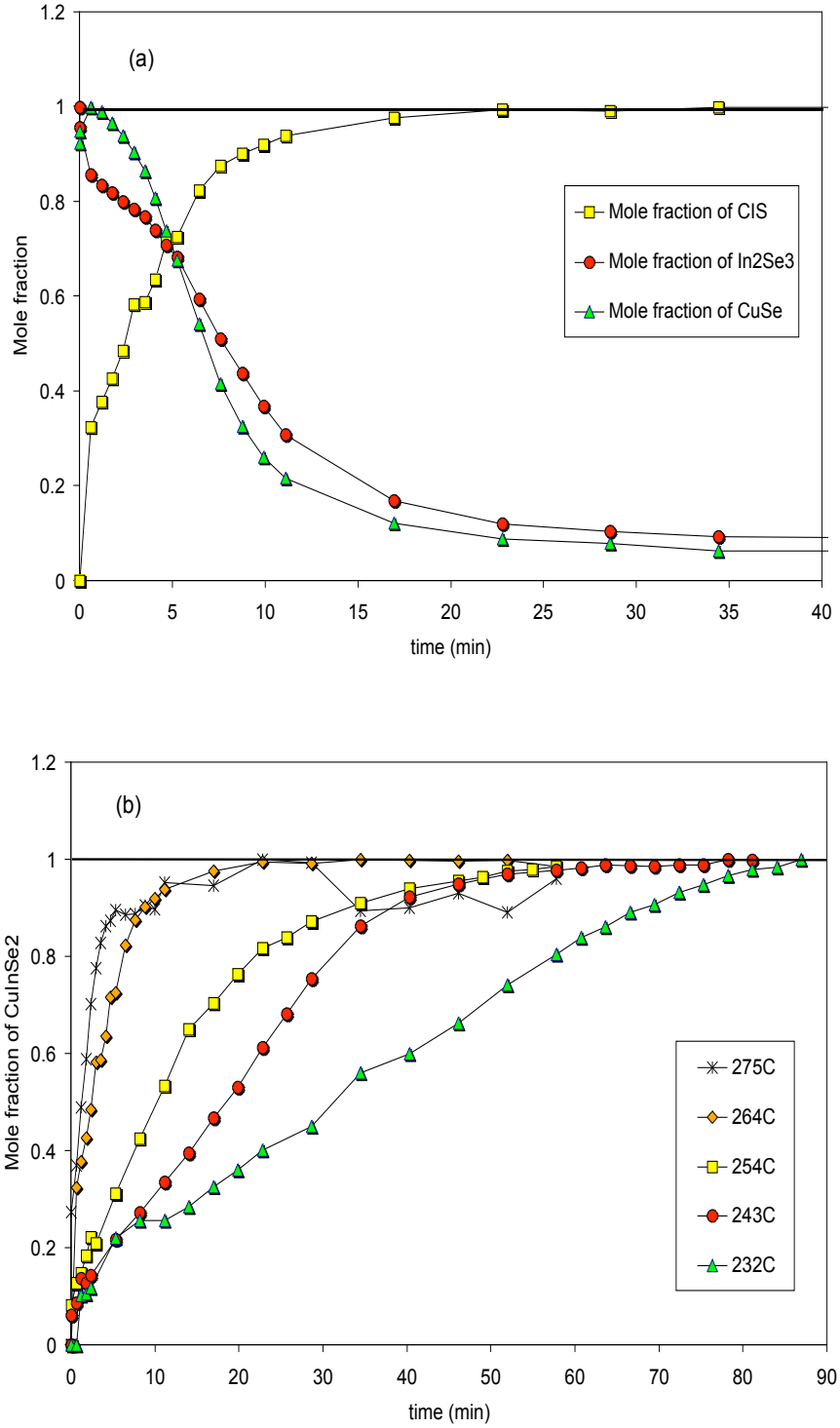

Figure 1-2. (a) Mole fraction changes of reactants (CuSe, In_2Se_3) and product ($CuInSe_2$) for isothermal reaction at 264°C. (b) Mole fraction change of $CuInSe_2$ as a function of time and temperature.

2 Progress on Growth of CIS Absorber Films and Thermal Modeling

Participants: Alex Chang (Faculty Advisor), Giang N. Ma (Graduate Research Assistant).

2.1 Objectives

Quantitative analysis of XAFS measurements using computer software to model theoretical parameters of the cadmium treated CIS samples (CIS:Cd).

2.2 Accomplishments during the current quarter

WinXAS data analysis program was employed to fit the experimental XAFS measurements of the local structure of cadmium in the CIS:Cd samples. Figure 2-1 illustrates a fit of the cadmium treated sample labeled 1852 at **low** $CdCl_2$ concentration. The blue theoretical curve was generated by using the space group I-42d to build the crystallographic structure of the CIS in the software. Then by relaxing the lattice with the simple space group P1; one oxygen atom replaced an indium atom (0.220, 0.250, 0.185), and two cadmium ions replaced selenium atoms [(1/2, 0, 1/4) and (1/2, 1, 1/4)] to simulate the cadmium treatment. The first shoulder peak represents the Cd-O bond with a nearest neighbor of 0.36 and 2.13 Å from each other. The second peak fit corresponds to the Cd-Se bond with a coordination number of 3.34 atoms at a distance of 2.62Å apart. These results are consistent with reported values although the Cd-O bond is noticeably different then 2.29Å reported by Carter *et al.* [1] Further investigation is needed to explain this occurrence.

2.3 Activities envisioned for the next quarter

FEFF analysis and fitting of the 1852 sample treated with a **higher** concentration of cadmium (1.5 M $CdCl_2$). We will try to reproduce the same fitting parameters as discussed above to determine the amount of Cd-O and Cd-Se interactions within this sample. Comparing and contrasting these results with those in Figure 1.1 may give insight to the variation seen in the Cd-O bond distance with reported values. This is not reported in this letter due to some contradictory results yet to be fully understood and explained. The difference in the fits is illustrated in Figure 2-2 of the two cadmium treated samples along with the bulk Cd-Se reference as reported last quarter. The reduction in the height and prominence in the first shoulder peak as the cadmium concentration increases may help describe the role of Cd-O, Cd-Se and/or Cd-OH bonds.

2.4 References cited

[1] A.C. Carter, C.E. Bouldin, K.M. Kemner and M.I. Bell, Phys. Rev. **55,** 13822 (1997).

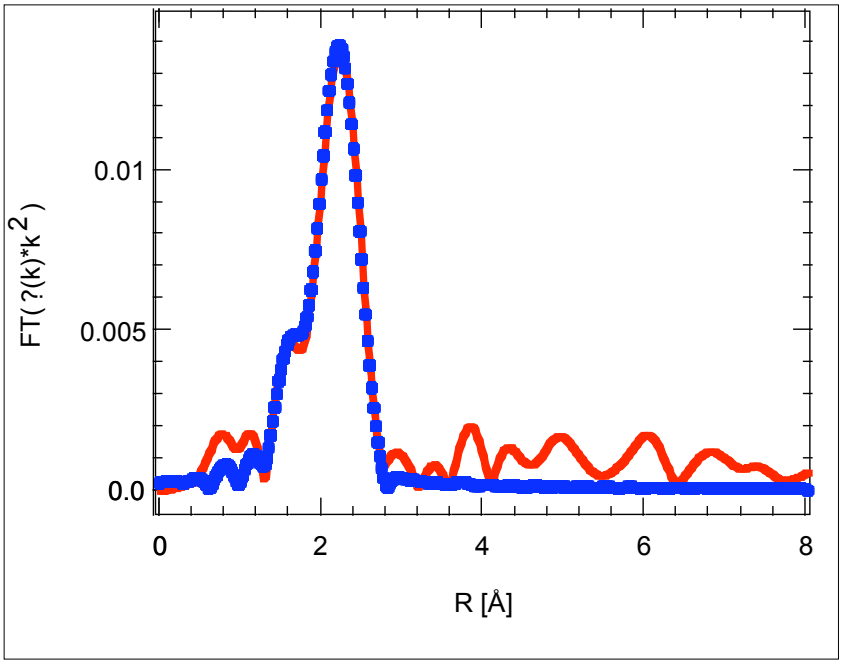

Figure 2-1. Quantitative fit of the 0.0015 M $CdCl_2$ treated sample labeled 1852. The red curve represents the experimental data, and the blue circles corresponds to the theorectical fit of the first shell in the CIS:Cd sample

3 Progress on the DLTS Characterization on CIGS Cells

Participants: Timothy J. Anderson (Faculty Advisor), Sheng S. Li (Faculty), Oscar D. Crisalle (Faculty) and Lei Li Kerr (Graduate Research Assistant)

3.1 Objectives

Use DLTS to determine the trap properties such as trap energy level, capture cross section, and trap concentration in the CIGS and provide fundamental knowledge of the defects as important inputs to develop meaningful device models.

3.2 Accomplishments during the current quarter

The DLTS and C-V measurements have been performed on a UF CIS sample and compared with the DLTS measurements on EPV and NREL CIGS samples. The defect activation energy and density were determined from these measurements. Table 3-1 summarizes the DLTS data on a 5% cell by RTP on bilayer precursor. In the UF CIS sample, a middle gap trap is detected and three other minority traps are also detected. The middle majority trap seems to be a dominant defect in the cell. This confirms the observation of the low V_{oc} in I-V curve. Therefore, in order to improve the cell efficiency, we still need to improve the junction quality by eliminating the middle gap defect. Adding Ga or S to create the bandgap gradient and adjust the Cu:In:Se composition ratio will be the reasonable methods. The EPV sample showed a majority carrier (hole) trap with activation energy and trap density determined. The NREL CIGS sample showed three minority carrier traps. Possible defect origins were depicted from this DLTS study. The results for samples from both locations are listed in Table 3-2. From the analysis in Table 3-1 and 3-2, we can conclude that V_{Se} and In_{Cu} are two main donor levels, V_{Cu} is the shallowest acceptor level, and Cu_{In} is the main middle level recombination center, which are consistent with the information from literature [1-3]. The free energy associated with the formation of some defect structures is so small that little increase in thermodynamic potential results and hence there is insufficient driving force to ensure their elimination under many synthesis conditions. The formation energy of these defects in CIS according to several authors' calculations are in the order of $V_{Cu}<In_{Cu}<Cu_{In} \approx In_{Cu} < V_{Se}$ [1,4]. However, the defect distribution largely depends on the composition.

3.3 References

[1] S.B. Zhang, S-H Wei, and A. Zunger, *Phys. Rev. B*, Vol 57, No. 16, pp 9642-9668, 1998.

[2] J.H. Schon and E. Bucher, *Solar Energy Materials & Solar Cells*, Vol. 57, pp. 229-237, 1999.

[3] H. Neumann and R.D. Tomlinson, *Solar Cells*, Vol. 28, pp.301-307, 1990.

[4] H. Neumann, G. Kuhn, and W. *Moller, Physica Status Solidi (b)*, Vol. 144, pp. 565, 1987.

Table 3-1. Summary of DLTS Data on UF CIS sample.

	V_R =-0.5 V V_H =0.4 V W= 10 ms	Cool to 77 K with reverse bias - 0.5 V, then apply V_R =-0.5V, V_H =0.7 V, W= 10 ms		Optical DLTS V_R =-0.5V λ=532 nm	
Approximate Peak Temperature (K)	290	290	200	150	300
DLTS peak Sign	-	-	+	+	+
Trap Carrier Type	Majority	Majority	Minority	Minority	Minority
Trap Activation Energy E_a (eV)	E_V +0.54	E_V +0.55	E_C -0.97	E_C - 0.16	E_C - 0.5 (?)
Trap Density(cm^{-3})	4.6×10^{12}	6.5×10^{12}	1.3×10^{12}	4.9×10^{12}	3.5×10^{13}
Possible Defect I.D.	Cu_{In}	Cu_{In}	V_{Cu}	In_{Cu}	Cu_{In}
Capture Cross Section σ (cm^2)	1.39×10^{-14}	5.7×10^{-15}		1.2×10^{-18}	

Table 3-2. Summary of DLTS and C-V data for the EPV and NREL samples.

	EPV CIGS	NREL CIGS		
Approximate Peak Temperature	270 K	100K	250 K	335 K
Activation Energy (eV)	E_v+0.94	E_c-0.067		
DLTS peak	-	+	+	+
Trap Carrier Type	Majority	Minority	Minority	Minority
N_a (cm^{-3})	3×10^{15}	2.25×10^{15}		
N_T (cm^{-3})	6.5×10^{13}	4.2×10^{13}		
Possible defect I.D.	V_{Se}	V_{Se}		
Capture Cross Section σ (cm^2)		6×10^{-18}		

4 Progress on Growth of CIS Absorber Films and Thermal Modeling

Participants: Rajiv K. Singh (Faculty Advisor), Valentin Craciun, Joshua Howard, and Seemant Rawal (Graduate Research Assistants)

4.1 Objectives

Activities for this quarter included additional laser anneals at fluences less than or equal to 50 mJ/cm^2 as supported by the previous findings. These were conducted on CdS buffer layers atop CIGS absorber cells with fluences of 30, 40, and 50 mJ/cm^2 and with fewer pulses.

4.2 Accomplishments during the current quarter

4.2.1 NLA experiments

Experimentation was conducted on CdS buffer layer atop CIGS absorber cells with the conditions shown in Table 4-1.

Table 4-1. Laser conditions for non-melt laser annealing.

Laser Condition	Fluence (mJ/cm^2)	Pulse Count
1	30	5
2	30	10
3	40	5
4	40	10
5	50	5
6	Control Sample	Control Sample

The samples were finished into devices and then characterized by current-voltage measurements and scanning electron microscopy (SEM) investigations. The efficiency of the samples was calculated and is shown in Figure 4-1. It is seen that the efficiency increases by nearly 4% after NLA treatment at the 30 mJ/cm^2 and 5 pulse condition.

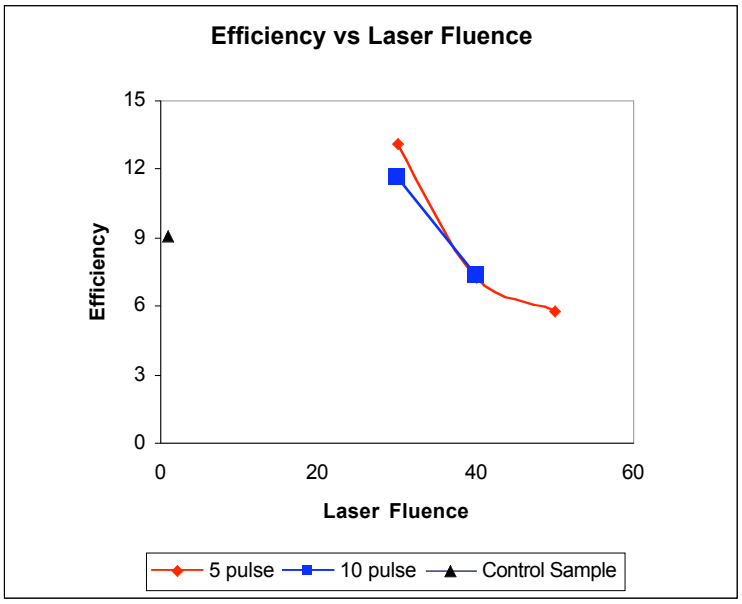

Figure 4-1. Efficieny vs. laser fluence for NLA treated CdS atop CIGS absorber cells.

While the NLA treatment at the 30 mJ/cm^2 and 10 pulse condition also resulted in a greater efficiency of the cell beyond the control sample, it is found that the larger number of pulses yielded a lower efficiency than the smaller number of pulses. Fluences greater than 30 mJ/cm^2 resulted in efficiencies lower than the control value indicating an overall degradation of the device as a consequence of NLA treatment. The important conclusion from the above experiments is that the optimum laser fluence/pulse condition for NLA treatment is 30 mJ/cm^2 and 5 pulses.

SEM was done on the both the NLA treated and non-treated samples and did not show significant changes in the morphology or grain size.

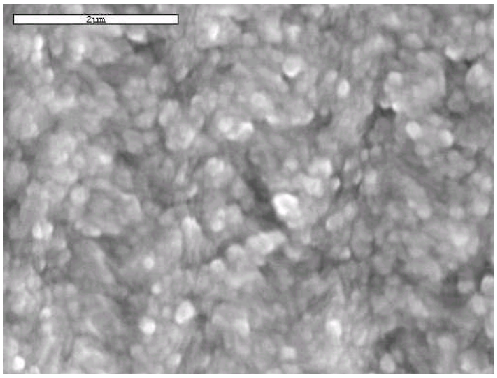

A) CdS: 20 mJ/cm2, 5 pulse

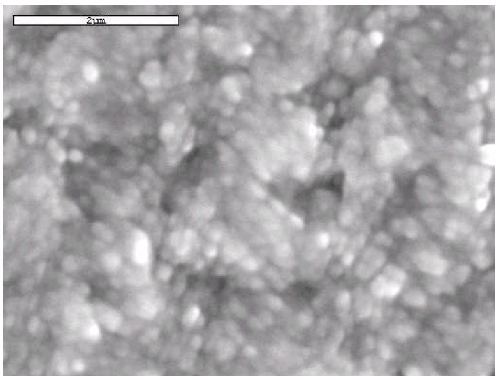

B) CdS: 20 mJ/cm2, 10 pulse

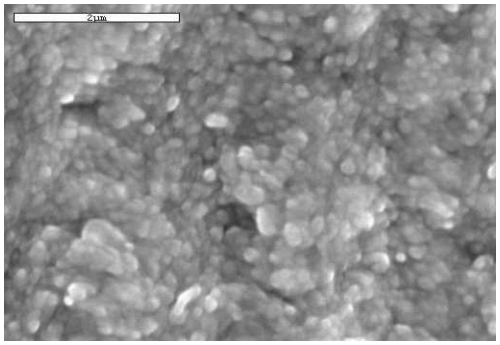

C) CdS: Not NLA treated

Figure 4-2. SEM images of NLA treated and non-treated samples.

4.3 Activities envisioned for the next quarter

Activities for the next quarter include additional non-melt laser anneals focusing on fluences just above and below 30 mJ/cm^2. The laser conditions in terms of laser fluence and pulses will also be optimized. Additionally, the samples will be treated by rapid thermal annealing (RTA) and a combination of RTA plus NLA. Experiments will be carried out to optimize the RTA conditions on the CIGS/CdS layer.

5 Investigation of Pulsed Non-melt Laser Annealing (NLA) of CIGS-Based Solar Cells

Participants: Sheng S. Li (Faculty Advisor), Xuege Wang, Lei Li Kerr, S. Rawal, J. M. Howard, V. Cracium, T. J. Anderson.

5.1 Objectives

The objective of this project is to study the effect of Non-melt Laser Annealing (NLA) on electrical and optical properties of the CIS/CIGS based solar cell, and to find the optimal laser condition in order to improve the cell's performance.

5.2 Accomplishments during the current quarter

Pulsed Non-melt Laser Annealing (NLA) has been used to modify the near surface defect density and related junction properties in CIGS solar cells. The previous research shows that low power NLA treatment could enhance the effective carrier lifetime, mobility, film grain size, and sheet resistance and lower the near-surface defect density in the films [1]. A new set of CIGS films deposited on Mo/glass substrates were annealed by the NLA technique at selected laser energy densities and pulse number, and fabricated into finished cells, and characterized by the photo I-V and Q-E measurements. The results suggest that low power NLA treatment could improve the I-V performance of CIGS cells.

5.2.1 The Photo- I-V results:

Six CIGS/CdS samples treated by NLA with different energy densities and pulse number were fabricated into finished devices. The NLA conditions and photo- I-V results of these samples are summarized in Table 5-1. Explicit improvements were found in the photo- I-V results of the annealed cells under 30mJ/cm^2, 5 pulses and 10 pulses NLA conditions. The data also show decreasing in all I-V performance parameters of the cells annealed by laser beam with energy density higher than 30mJ/cm^2. These results suggest that an optimal NLA energy density should be around 30 mJ/cm^2, 5 pulses. Figure 5-1 shows the trend of I-V parameters versus NLA condition. A slight increase of cell performance was found with NLA condition of 30mJ/cm^2, 5 pulses compared to the 10 pulses NLA cells.

Table 5-1. Photo- I-V results of NLA CIGS Solar cells.

Sample #	Voc (V)	Jsc(mA/cm^2)	F.F.(%)	Eff.%	NLA condition
CIGS/CdS #1	0.576	31.6	66.50	12.074	30mJ/cm^2, 5 pulses
CIGS/CdS #2	0.568	31.25	63.11	11.12	30mJ/cm^2, 10 pulses
CIGS/CdS #3	0.489	26.79	55.29	7.268	40mJ/cm^2, 5 pulses
CIGS/CdS #4	0.493	26.89	55.08	7.34	40mJ/cm^2, 10 pulses
CIGS/CdS #5	0.436	25.56	51.8	5.773	50mJ/cm^2, 5 pulses
CIGS/CdS #6	0.543	30.05	55.74	9.064	Control sample

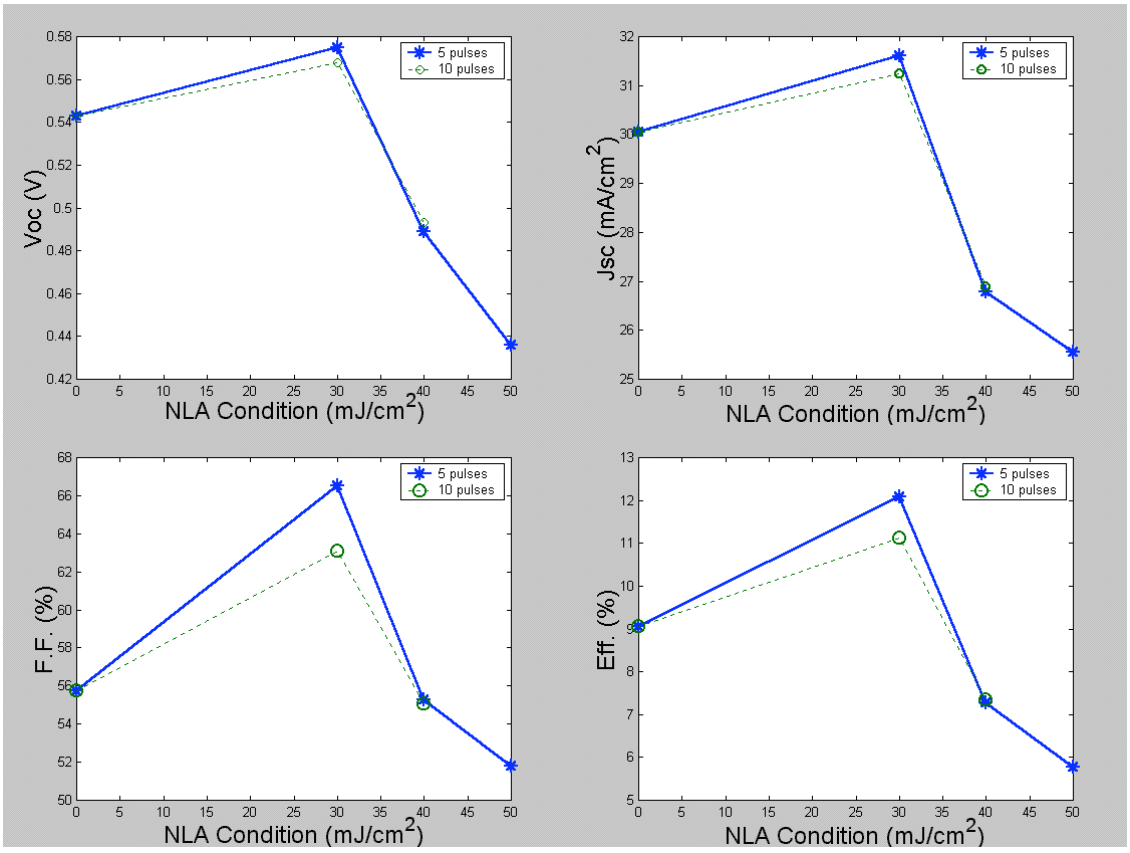

Figure 5-1. Voc, Jsc, Fill Factor and Conversion Efficiency versus different NLA condition.

5.2.2 Conclusions

The effect of pulsed NLA treatment on the CIGS-based solar cells was investigated under selected annealing conditions. Several characterization techniques (DBOM, XRD, SEM, Hall-effect, I-V and Q-E measurements) support the conclusion that pulsed NLA treatment under an optimal laser energy density condition can significantly improve the effective carrier lifetime, carrier mobility, surface morphology, spectral response (Q.E.) [1] and hence the cell performance. The energy density of the laser beam and the number of pulse cycle play a central role in modifying the optical and electrical properties of the CIGS absorbers.

5.3 Activities envisioned for the next quarter

Future efforts will be focusing on the optimization of pulsed NLA energy density and annealing cycle (based on near 30mJ/cm^2) for further improving the cell performance. A new set of experiments with NLA condition near 30mJ/cm^2 followed by both surface characterization and cell performance measurements under different annealing cycles will be included in the next quarterly report.

5.4 Publications and presentations

1. Xuege Wang, Sheng S. Li, C. H. Huang, Lei Li Kerr, S. Rawal, J. M. Howard, V. Cracium, T. J. Anderson, O. D. Crisalle, and R. K. Singh. "Investigation of Pulsed Non-melt Laser Annealing (NLA) of CIGS-Based Solar Cells", *the 3rd World Conference on Photovoltaic Energy Conversion* (WCPEC-3) (2003).

2. Xuege Wang, Sheng S. Li, C. H. Huang, Lei Li Kerr, S. Rawal, J. M. Howard, V. Cracium, T. J. Anderson, O. D. Crisalle, and R. K. Singh. "Investigation of Pulsed Non-melt Laser Annealing (NLA) of CIGS-Based Solar Cells", *the 2003 NCPV and Solar Program Review Meeting* (2003).

3. Xuege Wang, Sheng S. Li, C. H. Huang, Lei Li Kerr, S. Rawal, J. M. Howard, V. Cracium, T. J. Anderson, O. D. Crisalle, and R. K. Singh. "Investigation of Pulsed Non-melt Laser Annealing (NLA) of CIGS-Based Solar Cells", presented in poster session in *the 3rd World Conference on Photovoltaic Energy Conversion* (WCPEC-3) (2003).

4. Xuege Wang, Sheng S. Li, C. H. Huang, Lei Li Kerr, S. Rawal, J. M. Howard, V. Cracium, T. J. Anderson, O. D. Crisalle, and R. K. Singh. "Investigation of Pulsed Non-melt Laser Annealing (NLA) of CIGS-Based Solar Cells", presented at *the 2003 NCPV Review Meeting,* Denver, March 24-26 (2003).

5.5 References cited

[1] Xuege Wang, Sheng S. Li, C. H. Huang, Lei Li Kerr, S. Rawal, J. M. Howard, V. Cracium, T. J. Anderson, O. D. Crisalle, and R. K. Singh. "Investigation of Pulsed Non-melt Laser Annealing (NLA) of CIGS-Based Solar Cells", *the 3rd World Conference on*

Photovoltaic Energy Conversion (WCPEC-3) (2003).